HHS Public Access

Author manuscript

Biochim Biophys Acta. Author manuscript; available in PMC 2015 September 25.

Published in final edited form as:

Biochim Biophys Acta. 2013 December ; 1834(12): 2722–2728. doi:10.1016/j.bbapap.2013.09.007.

Comparison of the Catalytic Properties of the Botulinum Neurotoxin subtypes A1 and A5

Dongxia Wang[†], **Joan Krilich**[†], **Sabine Pellett**[‡], **Jakub Baudys**[†], **William H. Tepp**[‡], **John R. Barr**, **Eric A. Johnson**[‡], and **Suzanne R. Kalb**[†,*]

[†]Division of Laboratory Science, National Center for Environmental Health, Centers for Disease Control and Prevention, Atlanta, Georgia 30341, USA

[‡]Department of Bacteriology, University of Wisconsin-Madison, Madison, Wisconsin 53706

Abstract

Clostridium botulinum neurotoxins (BoNTs) cause the life-threatening disease botulism through the inhibition of neurotransmitter release by cleaving essential SNARE proteins. There are seven serologically distinctive types of BoNTs and many subtypes within a serotype have been identified. BoNT/A5 is a recently discovered subtype of type A botulinum neurotoxin which possesses a very high degree of sequence similarity and identity to the well-studied A1 subtype. In the present study, we examined the endopeptidase activity of these two BoNT/A subtypes and our results revealed significant differences in substrate binding and cleavage efficiency between subtype A5 and A1. Distinctive hydrolysis efficiency was observed between the two toxins during cleavage of the native substrate SNAP-25 versus a shortened peptide mimic. N-terminal truncation studies demonstrated that a key region of the SNAP-25, including the amino acid residues at 151 through 154 located in the remote binding region of the substrate, contributed to the differential catalytic properties between A1 and A5. Elevated binding affinity of the peptide substrate resulted from including these important residues and enhanced BoNT/A5's hydrolysis efficiency. In addition, mutations of these amino acid residues affect the proteolytic performance of the two toxins in different ways. This study provides a better understanding of the biological activity of these toxins, their performance characteristics in the Endopep-MS assay to detect BoNT in clinical samples and foods, and is useful for the development of peptide substrates.

1. Introduction

Clostridium botulinum produces seven serotypes of neurotoxins (A-G) distinguished by their antigenic properties(Schiavo, Matteoli et al. 2000). Exposure to botulinum neurotoxins (BoNTs) can cause a life-threatening disease in humans and animals, termed botulism, by targeting the soluble NSF attachment protein receptors (SNARE) complex proteins in the synaptic vesicle and plasma membranes of nerve cells. Cleavage of these important core components of the vesicular membrane fusion complex blocks the release of neurotransmitter molecules at neuromuscular junction and leads to discontinued nerve

[*]Corresponding author: Suzanne R. Kalb. SKalb@cdc.gov, phone: 770-488-7931. Fax: 770-488-0509.

Disclaimer: The findings and conclusions in this report are those of the authors and do not necessarily represent the official position of the Centers for Disease Control and Prevention.

impulse propagation and flaccid paralysis of muscle activity. Human botulism is usually caused by the serotypes A, B, E, and F (Werner, Passaro et al. 2000). The extreme toxicity and the ease of preparation make this toxin a potential agent for bioterrorism (Arnon, Schechter et al. 2001).

BoNTs are synthesized as a single chain protein consisting of a light chain of 50 kDa and a heavy chain of 100 kDa (DasGupta and Dekleva 1990). The heavy chain is responsible for receptor binding and membrane translocation. The light chain is a zinc-metalloprotease that cleaves one of the three SNARE complex proteins including Synaptosome-associated protein of 25 kDa (SNAP-25), synaptobrevin-2 (also termed VAMP 2) and syntaxin. BoNT/A, /E, and /C hydrolyze SNAP-25 at different locations near the C-terminal region of the protein (Blasi, Chapman et al. 1993; Blasi, Chapman et al. 1993; Schiavo, Rossetto et al. 1993; Binz, Blasi et al. 1994). BoNT/B, /F, /D, and /G target VAMP2 and cleave the substrate at distinct sites(Schiavo, Benfenati et al. 1992; Schiavo, Malizio et al. 1994; Yamasaki, Baumeister et al. 1994). Both SNAP-25 and syntaxin are targets of a BoNT/C endopeptidase (Blasi, Chapman et al. 1993; Foran, Lawrence et al. 1996). BoNTs are produced as non-covalently bound, high molecular weight complexes consisting of the toxin itself and several non-toxic neurotoxin-associated proteins; these prevent the toxin from degradation in the digestive tract(Collins and East 1998).

In addition to serologically distinct serotypes, many BoNT subtypes have been identified on the basis of their sequence variations and antigenic differences. Five subtypes (A1 through A5) of the type A botulinum neurotoxin have been identified through gene sequence analysis (Smith, Lou et al. 2005; Hill, Smith et al. 2007; Dover, Barash et al. 2009). While a sequence comparison among different serotypes yields relatively low homology, the subtypes within a BoNT serotype generally exhibit high sequence identity and similarity. At the amino acid level, the holotoxins BoNT/A1 through A4 display 76–95% sequence identity with each other (Arndt, Jacobson et al. 2006; Jacobson, Lin et al. 2011).

BoNTs' catalytic activity and substrate recognition have been extensively investigated (Binz, Sikorra et al. 2010). The peptide bond between Gln197 and Arg198 in the C-terminal SNAP-25 was determined to be the type A1 botulinum neurotoxin cleavage site (Blasi, Chapman et al. 1993). Later work has shown that the SNAP-25 cleavage site for A2, A3, A4, and A5 is also the same as for A1, between Gln197 and Arg198 (Henkel, Jacobson et al. 2009; Kalb, Lou et al. 2009; Jacobson, Lin et al. 2011). Deletion analysis suggested that the minimal region of SNAP-25 for effective cleavage by BoNT/A1 includes the residues 141–202(Washbourne, Pellizzari et al. 1997; Vaidyanathan, Yoshino et al. 1999). The residues at the position of 145–155 represent the region (exosite S4) of the conserved SNARE motifs of SNAP-25 that are important for substrate recognition(Rossetto, Schiavo et al. 1994). Co-crystal structure of an inactive BoNT/A1 light chain with a SNAP-25 peptide (146–204) revealed that SNAP-25 binds to the toxin's catalytic domain at the α-exosite remote from the protease's active site. (Breidenbach and Brunger 2004). The residues 147–167 of SNAP-25 form a distorted α-helix and interact with the enzyme at the interface of four BoNT/A1 light chain α-helices. Biochemical studies identified residues 156–202 of SNAP-25 as the optimal cleavage region for BoNT/A where residues 193–202 make up the active site domain and residues 156–181 form a binding domain. These two domains

contribute to cleavage capability and binding affinity, respectively(Chen and Barbieri 2006). Molecular modeling and biochemical studies suggest a multistep mechanism for the recognition of SNAP-25 by BoNT/A where initial binding of SNAP-25 along the belt region of BoNT/A prompts the proper docking of the key substrate residues into toxin's active site binding pockets and thus provide an optimal alignment of the scissile bond for cleavage(Chen, Kim et al. 2007).

Molecular modeling studies have suggested that sequence variations within the BoNT/A subtypes may impact their substrate binding affinity and cleavage efficiency. Using a peptide substrate in a mass spectrometric-based Endopep-MS assay, similar levels of C-terminal product were detected from the substrate cleavage by A1 and A2 while A3 and A4 showed relatively higher and lower yield of cleavage products, respectively(Kalb, Smith et al. 2008). Biochemical analysis using recombinant light chain of BoNT/A subtypes observed similar hydrolysis rates for full-lengthSNAP-25 cleavage by A1 and A2 and found similar binding affinity but different catalytic efficiency for the other two subtypes, A3 and A4 (Henkel, Jacobson et al. 2009).

The subtype BoNT/A5 has a very high sequence identity (97.1%) and similarity (97.9%) to the well-studied BoNT/A1 at the amino acid level (Carter, Paul et al. 2009; Jacobson, Lin et al. 2011). There are 36 amino acid differences between the two subtypes where most of them are located in the heavy chain and only 4 different amino acids (D102E, E171D, G268E and K381E) are found in the light chains with two conservative variations. The holotoxin protein of the subtype A5 was recently purified from *Clostridium botulinum* strain A661222 and shows a distinct difference in the antibody neutralization capacity from the subtype A1(Jacobson, Lin et al. 2011). In this study, we characterized the endopeptidase activity of the A5 subtype and reported the difference in substrate recognition between BoNT/A5 and BoNT/A1.

2. Materials and Methods

2.1. Chemicals

All chemicals were obtained from Sigma–Aldrich (St. Louis, MO) except where indicated otherwise. Fmoc-amino acid derivatives and peptide synthesis reagents were purchased from EMD Chemicals, Inc. (Gibbstown, NJ) or Protein Technologies (Tucson, AZ). Monoclonal antibodies were provided by Dr. James Marks at the University of California, San Francisco. Protein G coupled Dynabeads were purchased from Invitrogen (Lake Success, NY).

2.2. Preparation of botulinum neurotoxins

The 150 kDa proteins of BoNT/A1 and BoNT/A2 were purified from *C. botulinum* strains Hall A hyper and Kyoto F, respectively, as previously described(Malizio, Goodnough et al. 2000; Lin, Tepp et al. 2010). The BoNT/A5 complex was purified from *C. botulinum* strain A661222 as previously described(Jacobson, Lin et al. 2011). The toxins were stored in 40 % glycerol, 15 mM sodium phosphate, 90 mM NaCl at −20°C until use. The biological activity of the BoNT/A preparations was determined by the mouse bioassay (Schantz and Kautter 1978; Hatheway 1988), and specific toxicity was about 1.3×10^8 mouse LD50 Units/mg for

BoNT/A1, 4.3×10^8 mouse LD50 Units/mg for BoNT/A2, and 1.5×10^7 mouse LD50 Units/mg for BoNT/A5.

2.3. Peptide synthesis

All peptides were prepared in house by a solid phase peptide synthesis method using Fmoc chemistry on a Tribute peptide synthesizer (Protein Technologies, Tucson, AZ, USA) or a Liberty microwave peptide synthesizer (CEM, Matthews, NC, USA). Peptides were cleaved and deblocked using a reagent mixture of 95% trifluoroacetic acid (TFA): 2% water: 2% anisole: 1% ethanedithiol and purified by reversed-phase HPLC using a water: acetonitrile: 0.1% TFA gradient. Correct peptide structures were confirmed by matrix-assisted laser desorption/ionization time-of-flight (MALDI TOF) mass spectrometry (MS). All peptides were dissolved in deionized water as a 1 mM stock solution and were stored at −70°C until further use.

2.4. Activity assay

In-solution or on-bead endopeptidase activity assays were carried out as previously described (Wang, Baudys et al. 2011). In brief, the reaction was conducted in a 20 μL reaction volume containing SNAP-25 or peptide substrates with indicated concentration, 10 μM $ZnCl_2$, 1 mg/mL BSA, 10 mM dithiothreitol, and 200 mM HEPES buffer (pH 7.4) at 37°C for various lengths of time as indicated in the text. For the in-solution assays without antibody-coated beads, 1 nM BoNT/A1, /A2, or /A5 was directly added into the reaction mixture. For the on-bead assay, the toxin spiked into 0.6mL of phosphate buffered saline with 0.05%Tween-20 was first purified by antibodies immobilized on Protein-G beads followed by immersing the beads into the 20 μL reaction solution for the assay as described above. After the completion of the cleavage reaction, 2 μL of the supernatant was mixed with 2 μL of a 0.5 μM internal standard peptide (IS, RATKML(+7)GSG, 927.5Da) and 16 μL of α-cyano-4-hydroxy cinnamic acid (CHCA) at 5 mg/mL in 50% acetonitrile/0.1% TFA/1 mM ammonium citrate. The formation of cleavage products was measured as the ratio of the isotope cluster areas of the MS peak of the C-terminal product (A_{CT}) versus an internal standard (A_{IS}). The amount of the cleavage product (CT) was determined by multiplying the concentration of added IS by the ratio of A_{CT} over A_{IS}. Each sample was spotted in triplicate on a MALDI plate and analyzed on an Applied Biosystems 4800 or 5800 MALDI-TOF instrument (Framingham, MA). Mass spectra of each spot were obtained by scanning from 800 to 3000 *m*/*z* in MS-positive ion reflector mode. The instrument uses a Nd-YAG laser at 355 nm, and each spectrum is an average of 2400 laser shots. The data were usually an average of three experiments with a CV below 20%.

2.5. Kinetic assay

Cleavage reactions containing 1 or 2 nM of the BoNT/A subtypes and SNAP-25 or peptide substrates with indicated starting concentrations of substrate were performed to determine initial velocities. The formation of cleavage products was controlled to be less than 10% of the substrate amount used. Aliquots from the reaction solution were removed at 2, 4, 6, 8, and 10 min or indicated time points to obtain a time-course response. Initial velocities were measured as the slopes of the product versus time plots. The kinetic constants were derived

by fitting the data of initial velocity versus substrate concentration to the Michaelis-Menten equation shown below using the JMP10 program (SAS Institute, Cary, NC).

$$\upsilon = -\frac{V_{max}[S]}{K_m + [S]}, \quad V_{max} = k_{cat}[E]_0$$

Here υ represents the reaction rate; [S] and $[E]_0$ represent the concentration of substrate and enzyme, respectively. V_{max} is the maximum rate achieved by the system at saturating substrate concentrations. K_m is the substrate concentration at which the reaction rate is half of V_{max}, k_{cat} denotes the rate constant or turnover number.

2.6. 1D Gel electrophoresis

SDS-PAGE gel electrophoresis was performed on a NuPAGE Novex Bis-Tris gel following the standard procedure (Invitrogen, Carlsbad, CA). In brief, 1–2 μg of the sample was added into 10 μL of 1X sample buffer and heated at 90 °C for 10 min. The proteins were loaded on a 4–12% gradient gel and the gel was run at 200V for 45 min. The finished gel was stained with coomassie blue dye (Thermo Fisher, Rockford, IL) following manufacturer's protocol.

3. RESULTS

3.1. Cleavage of SNAP-25 or peptide substrates by the botulinum neurotoxin A subtypes

To examine the hydrolysis of protein or peptide substrates by BoNT/A subtypes, we conducted *in vitro* activity assays where the toxin and substrate were incubated in the reaction buffer and the cleavage product was monitored by MALDI TOF MS. Two different substrates were initially examined: a recombinant native substrate, full-length SNAP-25, and a short peptide substrate, Peptide 1 (Scheme 1). Peptide 1 was derived and optimized from SNAP-25's C-terminal sequence surrounding the BoNT/A cleavage site and is used as the substrate in a mass spectrometry-based Endopep-MS assay(Wang, Baudys et al. In press). The full-length subtype A1 and A2 were purified as a single neurotoxin protein while the subtype A5 was prepared as a complex including its associated proteins (Figure 1, lanes 2–4). Equivalent amount of the toxins based on moles of toxin were used in each experiment. As shown in Table 1, the linear cleavage rates of A1 and A2 displayed a similar trend for both protein and peptide substrates where A1 had slightly higher hydrolysis efficiency than A2 did. In contrast, A1 and A5 demonstrated different relative cleavage efficiency when comparing SNAP-25 to the peptide substrate. BoNT/A1 showed almost equal efficiency in cleaving SNAP-25 and peptide 1; BoNT/A2 had a slightly better hydrolysis rate for peptide 1 than SNAP 25, which was only half the hydrolysis rate of BoNT/A1; BoNT /A5 had a greater hydrolysis rate than A1 for SNAP-25 but a lower hydrolysis rate for peptide 1. In other words, A1 is more efficient than A5 in the cleavage of Peptide 1 but had a lower rate of hydrolysis of SNAP-25. In an attempt to understand the underlying mechanism of this variance between A1 and A5, we conducted kinetic analysis by measuring the velocity of the product formation with various concentrations of the substrates under different time points and then fitting the data to the Michaelis-Menten equation (Figure 2). The k_{cat} values were similar for the proteolysis of SNAP-25 by A1 and A5 but the K_m of the A1 cleavage

was approximately two-fold higher than that of the A5 reaction, resulting in a higher overall catalytic efficiency of A5 for the native substrate, SNAP-25 (Table 2). For Peptide 1, however, the K_m values were similar but the k_{cat} for A1 was greater than that for A5. This result revealed that it was the difference in the SNAP-25 binding affinity that contributed to the differential cleavage efficiency between A1 and A5.

The Endopep-MS assay to detect BoNT in complex matrices such as clinical samples (serum, stool extracts, gastric extracts, and culture supernatants derived from clinical samples) and foods uses immunomagnetic extraction of the toxins so the activity assays were also performed with the A5 captured on a toxin-specific antibody immobilized on magnetic beads. The immunomagnetic extraction of the toxins with extensive washing largely removes the associated non-toxin proteins present in the A5 complex. The associated proteins present in lane 4 of Figure 1 of the A5 complex were not visualized in lane 6, where a sample following antibody capture was loaded. The two bands at approximately 155 kDa and 15 kDa represent protein components associated with antibody-coated streptavidin beads antibody used to capture BoNT/A toxins in the experiment. This was confirmed by comparing lane 6 with lane 5 where the pure BoNT/A1 (lane 2, without antibody capture) was first captured on the antibody-beads under identical experimental conditions. In addition, the two bands were not present in the gel of the control sample without addition of BoNT/A toxin (data not shown). The kinetic constants of the reaction of SNAP-25 with such purified A5 were determined to be only slightly lower than the ones measured with the A5 complex, suggesting that under the conditions used in this study the associated proteins in the A5 complex did not significantly affect the catalytic efficiency of the toxin (Table 2). The difference in A1 and A5 for the cleavage of the native protein and peptide substrates should be attributed to their intrinsic catalytic properties.

A product inhibition study was conducted to decipher the molecular mechanism behind the differential endopeptidase activities between A1 and A5. The assay was run by adding various concentrations of purified N-terminal cleavage product (NT-SNAP-25) as an inhibitor to the hydrolysis reaction solution. The external NT-SNAP-25 should not interfere with the mass spectrometric measurement of the cleavage product as it was determined by monitoring the formation of the C-terminal product and not the N-terminal one. Significant reduction of the formation of the C-terminal cleavage product was observed with increasing NT-SNAP-25 concentrations and 50% inhibition was reached at approximately 0.5 μM of the NT-SNAP-25 (Figure 3), similar to the amount of the product yielded at the 30 μM concentration of SNAP-25, a starting point for the rate decline (Figure 2B). This result verified that reduced cleavage at the high SNAP-25 concentration in the kinetic analysis study was caused by product inhibition. It was interesting to observe that no further inhibition occurred at higher than 0.6 μM of NT-SNAP-25 added in both A1 and A5 hydrolysis reactions but the maximum inhibition effects were not the same for the A1 (~ 80%) and A5 (~95%). This is consistent with the observation that occurred in the kinetic analysis, where A5 hydrolysis has a steeper rate of decline than the A1 reaction at the high concentration of SNAP-25 substrate (Figure 2B).

3.2 Substrate determinant for enhanced cleavage efficiency of BoNT/A5

To determine the specific region or residues in the N-terminal portion of SNAP-25 substrate that may contribute to the differential substrate binding capacity to BoNT/A1 and BoNT/A5, a series of synthetic peptides were prepared and their activity as a peptide substrate was examined. Each peptide was designed to be truncated at various N-terminal positions of SNAP-25 while its C-terminal sequence including the BoNT/A cleavage site remained untouched. The longest peptide, 141–206, includes a previously determined minimal region of SNAP-25 (residues 141–202) that is required for the effective cleavage by BoNT/A1 (Washbourne, Pellizzari et al. 1997; Vaidyanathan, Yoshino et al. 1999). The shortest one, 171–206, contains the amino acids consisting of the optimal active domain for BoNT/A1 hydrolysis(Chen and Barbieri 2006). Table 3 shows the hydrolysis rate of these N-terminal truncated SNAP-25 peptides cleaved by BoNT/A1 and /A5, respectively. For the peptides truncated at the position of 156 or higher (156–206, 161–206, 171–206), both A1 and A5 had higher rates of cleavage as the peptides became longer but, A1 displayed much higher cleavage rates than A5. In contrast, the catalytic efficiency of A5 was enhanced drastically from 0.014 to 0.097 when the peptide sequence extended to the position of 151 (151–206) in comparison to the performance of peptide 156–206, while the cleavage of the two peptides by A1 remained unchanged. This led to a substantial increase in the relative hydrolysis rates of A5 versus A1 from 0.7 to 5.5 for 156–206 and 151–206, respectively. Further extension of the peptide (146–206) produced a similar individual and relative cleavage rate. Taken together, these data demonstrated that a partial or complete sequence region of the amino acid residues 151 to 155 ($E_{151}Q_{152}V_{153}S_{154}G_{155}$) directly contributed to the changes of the hydrolysis rates between BoNT subtypes A1 and /A5. The presence of this region in the peptide substrates facilitated their cleavage by BoNT subtype A5 to a significantly higher extent than by A1 subtype through increased binding affinity.

To further pinpoint the residue(s) responsible for elevated cleavage efficiency of BoNT/A5, we prepared another set of truncated peptides where a single N-terminal residue was sequentially removed from the 151–206 to form four new peptides including 152–206, 153–206, 154–206 and 155–206. Table 3 showed that the peptide 155–206 resulted in a relative cleavage rate (0.8) similar to the value of 156–206 (0.7) for A5, suggesting the residue G155 might not be among the key players for A5's activity enhancement. Meanwhile, the ratio of the cleavage rates increased gradually from 0.8 to 2.2 as additional N-terminal residues were added, revealing that the E151, Q152, V153 and S154 were important amino acid residues for enhancing A5's catalytic activity and distinguishing it from A1. The residues Q152 and E151 were the two residues that showed the greatest enhancement for A5 cleavage.

3.3. Mutations on peptide substrates alter the toxin's catalytic properties

Before the experiments with single amino acid truncation in the region of 152 through 155 were conducted, we initially postulated that the residue S154 of SNAP-25 might be a candidate for altering A5's catalytic property. The crystal structure of BoNT/A and SNAP-25 peptide complex revealed that S154 is proximate to the D102 of BoNT/A1 (Figure 4)(Breidenbach and Brunger 2004). One of the four variations between A1 and A5 light chains is the substitution of aspartic acid (D) at 102 in A1 with the glutamic acid (E) in A5, another acidic residue that is one methylene group shorter than the former. We prepared four

single-point mutants based on the sequence of the peptide 153–206 with alanine, homoserine (hS), lysine or arginine incorporated at the position 154. The peptide S154A was designed to remove the polar hydroxyl group from the serine side chain so that the theoretical interaction of S154 and E102 of A5 could be disrupted whereas the homoserine in the S154hS, one methylene group longer than serine, could compensate the length difference between the side chains of A1's D102 and A5's E105 and form a novel peptide-A1 interaction similar to the one proposed for A5. The peptides S154K and S154R were constructed to examine whether an ionic interaction could be formed between the positively charged Lys and Arg in the peptides with the negatively charged D or E in the toxin. Compared with the wild type peptide 153–206, the mutant S154A, however, did not induce significant decline in its cleavage by A5 and there was not any significant increase in the cleavage efficiency of the S154hS by A5 (Table 3). As a consequence, their relative cleavage efficiency remained unchanged, suggesting that S154 does not have direct interaction with the E102 of A5. The cleavage rates of S154K and S154R mutants did increase significantly for both toxin subtypes, three-fold for A1 and two-fold for A5. Since the increase in hydrolysis rate of the S154K and S154R mutants increased more for A1 than for A5, the differences in the hydrolysis rate was from a relative ratio of A5/A1 cleavage efficiency of 1.5 for S154 to 0.9 or 1.0 for S154K and S154R mutants respectively. The activity variation of the two BoNT/A subtypes was diminished by these S154K and S154R mutations which implies that the positively charged group at substrate position 154 formed new interaction(s) with an unknown residue(s) of the catalytic domains in both A1 and A5.

The valine residue at the position 153 of SNAP-25 is located in the helical region and was directly involved in the hydrophobic interaction with A1's catalytic domain at the α-exosite in the structure of inactive A1 and substrate complex (Figure 4) (Breidenbach and Brunger 2004). Our truncation study determined it was an important residue in promoting A5's endopeptidase activity. To further investigate the function of this specific residue, four peptide mutants (V153A, V153K, V153D, and V153E) with single residue substitution on the template peptide 153–206 were prepared. Compared with the wild type, a conservative mutation in the V153A yielded slightly improved cleavage by A1 and no significant change for A5, suggesting the contact environment for residue 153 might remain unchanged (Table 3). In contrast, the peptide containing a distinctive mutation with a basic lysine residue (V153K) increased the A1 substrate cleavage four times while only a two-fold increase was detected in the hydrolysis rate of A5, leading to a decrease of the relative cleavage rate from 1.5 to 0.7. This effect was similar to the described outcome of the S154 mutant and prompted us to examine another residue flanking the other side of the serine residue. Replacement of G155 on the 153–206 peptide again demonstrated higher cleavage rates for both A1 and A5 and a lower relative rate ratio (0.9). These results suggested that the basic residues like lysine or arginine in these mutants directly contact either a single or multiple counterparts in the catalytic domain of the toxins through a salt bridge or other route. In addition, the comparable cleavage rates of A1 (0.060 – 0.076) and A5 (0.053 – 0.060) on these mutated peptides suggest that novel enzyme substrate interaction(s) might overcome the differentiating effect caused by one or more of the four amino acid variations between the light chains of A1 and A5.

In contrast to the effect of basic amino acid mutation, substitution of the V153 with an acidic residue, aspartic acid or glutamic acid, generated different consequences. The hydrophobic interaction between V153 and its corresponding counterpart in A1 should be negated by such mutations. Instead, the hydrolysis cleavage rate of A5 increased by approximately two-fold using V153D or V153E as its substrate, while a slight reduction in A1 cleavage was observed, resulting in a significant expansion of the relative cleavage efficiency (4.0 or 3.2) between A5 and A1 (Table 3). Negatively charged residues in position 153 might interact directly with an unknown residue of A5 and enhance the binding affinity of the peptide mutants. As previously described, the presence of the N-terminal acidic glutamic acid residue, E151, in the peptide 151–206 raised the cleavage rate of both A1 and A5 and the relative cleavage efficiency as well, as compared with the peptide 152–206. The difference in cleavage efficiency of A5 between the peptide 151–206 and the peptide V153D or V153E suggest that it is unlikely that the same residue(s) in the A5 light chain contact the carboxylic side chain of E151 and that of D153 or E153 in the mutated peptide. The hydrolysis of a new peptide mutant (E151A) provided supporting information where the replacement of the carboxyl group with a nonpolar side chain in alanine resulted in an A5 cleavage rate higher than those yielded from the peptides V153D and V153E. Further structure-activity studies are required to address the molecular mechanism of difference of A1 and A5 in the substrate binding at the α-exosite.

4. DISCUSSION

Among the five identified BoNT/A subtypes, the light chains or catalytic domain (1–437) of BoNT/A5 and BoNT/A1 are the most similar (Arndt, Jacobson et al. 2006). Only 4 amino acids (D102E, E171D, G268E and K381E) in the catalytic domains are different and two of these changes are conservative substitutions. This high degree of homology led us to expect that the light chains of the two BoNT/A subtypes should adapt a very similar three-dimensional structure and catalytic property. Surprisingly, different cleavage performances of the two subtypes were observed when the full length native protein substrate and a short peptide were examined. While A1 hydrolyzed the peptide substrate more efficiently, A5 was more efficient with the native protein substrate due to the different substrate binding affinities (Table 2).

A remote substrate binding site (α-exosite) away from the active site of the BoNT/A light chain was revealed by the co-crystal structure of an inactive BoNT/A1 with a SNAP-25 peptide (141–204) (Breidenbach and Brunger 2004). The α-helix (147–167) of the substrate involved in direct contact with a specific region of the BoNT/A1 catalytic domain formed from the α5 through α8 helices in the α-exosite (Figure 4). In the present study, the short substrate, Peptide 1, lacking the amino acid residues that form the α-helix at 147–167 should not be able to interact with the enzyme at the α-exosite in the same way as the full length SNAP-25. Therefore, the difference in the catalytic properties of A1 and A5 is likely to be associated with altered α-exosite interactions between substrate and toxin. Further investigation with N-terminal truncated peptides demonstrated that a specific amino acid region of 151–154 within the α-helix of the SNAP-25 contributed to the favorable binding of the substrate to BoNT/A5. To the best of our knowledge, the effect and importance of the region 151–155 of the SNAP-25 substrate on the cleavage by BoNT/A subtypes has not

been previously described. Although the present work was not able to identify the structural mechanism for these differentiated catalytic properties between the two BoNT/A subtypes, we can speculate that the conservative change of the amino acid at the 102 position (Asp to Glu) and/or the non-conservative variation at 268 (Gly to Glu) in A5 might play a role in altering the local structure and interactions at the α-exosite because these are two residue changes in or near the remote substrate binding site. Whether the entire or only a partial network of the substrate-enzyme interactions at the α-exosite varies between the two BoNT/A subtypes is a question that needs to be addressed. The cleavage rates of peptide 156–206, which included residues for a portion of the substrate α-helix, increased to a similar extent for both A1 and A5 as compared to that of peptide 161–206, where five helix residues were omitted, suggesting that the exosite interactions with the partial substrate helix might be the same for the two enzymes. Further investigation is needed to uncover the difference in the α-exosite interactions for these two toxin subtypes.

In a biochemical study of the substrate recognition by BoNT/A, Chen *et al* used deletions in SNAP-25 to identify the SNAP-25 region of 156–202 as the optimal domain, including the exosite binding and the cleavage site (Chen and Barbieri 2006). A consistent result for BoNT/A1 was obtained in the present study in which five additional N-terminal residues in peptide 156–206 versus the 161–206 achieved a dramatic improvement in substrate hydrolysis. On the other hand, further extension in the N-terminal part of a peptide substrate, such as in the peptides 151–206 through 146–206, did not make any significant changes in their cleavage rates. However, in the case of A5, an additional six-fold increase in hydrolysis of the peptide 151–206 over that of the peptide 156–206 suggests that the extension of the optimal domain should be considered for the development of a substrate and inhibitor suitable for both BoNT/A subtypes, and that the optimal domain may differ for additional not yet studied subtypes.

A mutation study on the key residues of the peptide showed that among the four residues that differ in the catalytic domain of A1 and A5, one (D102 in A1) is located within the α1 helix that participates in the enzyme-substrate interactions in the α-exosite, as shown in the crystal structure of the complex (Figure 4) (Breidenbach and Brunger 2004). Because the side chain of the E102 in A5 is one carbon longer than the D102 in A1, we initially assumed that it forms some kind of direct interaction with the residue(s) at S154 or V153 while the D102 in A1 may not be long enough to form such an interaction. Experiments with the S154hS peptide designed to compensate the difference in the side chains of D102 in A1 and E102 in A5 did not support this hypothesis. Neither the individual cleavage rates of the S154hS by A1 and A5 nor the relative rate ratio for the two toxins changed compared to the wild type peptide. However, it is interesting to observe that the substitution of the serine with lysine or arginine, a basic residue, altered the catalytic efficiency of A1 and A5 as well (Table 3). The hydrolysis rates for both toxins were enhanced, but a higher increase for A1 than for A5 was detected and this consequently reduced the difference of their relative hydrolysis efficiency. A similar phenomenon was observed on the cleavage of the other two mutants where two different residues (V153 and G155) adjacent to S154 were replaced by a lysine reside individually. Although the residues of S154 and G155 lie in the middle of the substrate α-helix and their hydrophilic side chains were projected towards the solvent in the

BoNT/A1 and substrate complex, the end location of S154K and G155K in the peptide mutants might make the side chains of the basic residues flexible enough to twist or turn toward the enzyme residues and form direct contact. Other interesting results were generated from the mutation of the valine residue at the position 153. When the residue was replaced with aspartic acid or glutamic acid, negative charge acidic residues, the A5 enzyme displayed even higher activity than A1 and further increased the difference of the hydrolysis efficiency between these two toxins (Table 3). These discoveries provide insight on the understanding of the underlying mechanisms of substrate binding and catalysis for the BoNT/A subtypes as well as for developing a better peptide substrate for toxin detection and inhibition studies.

5. CONCLUSION

The recently discovered BoNT/A subtype A5 has a very high sequence similarity and identity with the intensely studied subtype A1. Only four of 437 amino acid residues, including two conservative variations, differ in the catalytic domains or light chains that govern the endopeptidase activity of these two toxins. Despite their extremely high sequence homology, we demonstrated that the two toxin subtypes displayed different catalytic properties for cleavage of a full length SNAP-25 and a shortened peptide substrate. Truncation studies revealed a key region of SNAP-25, including the amino acid residues at 151 through 154, that contribute to the differential catalytic efficiency. The enhancement of the A5 hydrolysis efficiency is likely due to altered enzyme-substrate interactions at the remote substrate binding site, or α-exosite, but not at the active site of the catalytic domain. Our data showed that some mutations of these important A5-favored residues affect the hydrolysis performance of these two BoNT/A subtypes in different ways. These findings provide useful information for understanding the molecular mechanism of substrate recognition for various BoNT/A subtypes and for developing an optimal peptide substrate for toxin detection and inhibition.

ABBREVATIONS

BoNT/A	botulinum neurotoxin serotype A
LC	light chain
NSF	N-ethylmaleimide-sensitive factor
SNARE	soluble NSF attachment receptor
SNAP-25	soluble NSF attachment protein 25
VAMP2	vesicle-associated membrane protein 2
D	aspartic acid
E	glutamic acid
A	alanine
V	valine
hS	homoserine

S	serine
Q	glutamine
G	glycine
K	lysine
R	arginine
MS	mass spectrometry

References

Arndt J, Jacobson M, et al. A structural perspective of the sequence variability within botulinum neurotoxin subtypes A1-A4. Journal of Molecular Biology. 2006; 362(4):733–742. [PubMed: 16938310]

Arnon SS, Schechter R, et al. Botulinum Toxin as a Biological Weapon. JAMA: The Journal of the American Medical Association. 2001; 285(8):1059–1070. [PubMed: 11209178]

Binz T, Blasi J, et al. Proteolysis of SNAP-25 by types E and A botulinal neurotoxins. Journal of biological chemistry. 1994; 269(3):1617–1620. [PubMed: 8294407]

Binz T, Sikorra S, et al. Clostridial neurotoxins: mechanism of SNARE cleavage and outlook on potential substrate specificity reengineering. Toxins. 2010; 2(4):665–682. [PubMed: 22069605]

Blasi J, Chapman ER, et al. Botulinum neurotoxin A selectively cleaves the synaptic protein SNAP-25. Nature. 1993; 365(6442):160–163. [PubMed: 8103915]

Blasi J, Chapman ER, et al. Botulinum neurotoxin C1 blocks neurotransmitter release by means of cleaving HPC-1/syntaxin. EMBO journal. 1993; 12(12):4821–4828. [PubMed: 7901002]

Breidenbach MA, Brunger AT. Substrate recognition strategy for botulinum neurotoxin serotype A. Nature. 2004; 432(7019):925–929. [PubMed: 15592454]

Carter A, Paul C, et al. Independent evolution of neurotoxin and flagellar genetic loci in proteolytic Clostridium botulinum. BMC genomics. 2009; 10:115–115. [PubMed: 19298644]

Chen S, Barbieri J. Unique substrate recognition by botulinum neurotoxins serotypes A and E. Journal of biological chemistry. 2006; 281(16):10906–10911. [PubMed: 16478727]

Chen S, Kim J-J, et al. Mechanism of substrate recognition by botulinum neurotoxin serotype A. Journal of biological chemistry. 2007; 282(13):9621–9627. [PubMed: 17244603]

Collins MD, East AK. Phylogeny and taxonomy of the food-borne pathogen Clostridium botulinum and its neurotoxins. Journal of applied microbiology. 1998; 84(1):5–17. [PubMed: 15244052]

Copeland, RA. Enzymes: A Practical Introduction to Structure, Mechanism, and Data Analysis. New York: Wiley-VCH, Inc; 1996.

DasGupta BR, Dekleva ML. Botulinum neurotoxin type A: sequence of amino acids at the N-terminus and around the nicking site. Biochimie. 1990; 72(9):661–664. [PubMed: 2126206]

Dover N, Barash J, et al. Novel Clostridium botulinum toxin gene arrangement with subtype A5 and partial subtype B3 botulinum neurotoxin genes. Journal of clinical microbiology. 2009; 47(7): 2349–2350. [PubMed: 19420169]

Foran P, Lawrence GW, et al. Botulinum neurotoxin C1 cleaves both syntaxin and SNAP-25 in intact and permeabilized chromaffin cells: correlation with its blockade of catecholamine release. Biochemistry. 1996; 35(8):2630–2636. [PubMed: 8611567]

Hatheway, CL. Laboratory diagnosis of infectious diseases: principles and practice. Botulism, BA.; HWH, OM.; TMA, editors. New York: Springer-Verlag; 1988. p. 111-133.

Henkel J, Jacobson M, et al. Catalytic properties of botulinum neurotoxin subtypes A3 and A4. Biochemistry. 2009; 48(11):2522–2528. [PubMed: 19256469]

Hill KK, Smith TJ, et al. Genetic diversity among Botulinum Neurotoxin-producing clostridial strains. Journal of bacteriology. 2007; 189(3):818–832. [PubMed: 17114256]

Jacobson M, Lin G, et al. Purification, modeling, and analysis of botulinum neurotoxin subtype A5 (BoNT/A5) from Clostridium botulinum strain A661222. Applied and environmental microbiology. 2011; 77(12):4217–4222. [PubMed: 21515732]

Kalb S, Lou J, et al. Extraction and inhibition of enzymatic activity of botulinum neurotoxins/A1, /A2, and /A3 by a panel of monoclonal anti-BoNT/A antibodies. PLoS ONE. 2009; 4(4):e5355–e5355. [PubMed: 19399171]

Kalb S, Smith T, et al. The use of Endopep-MS to detect multiple subtypes of botulinum neurotoxins A, B, E, and F. International journal of mass spectrometry. 2008; 278(2–3):101–108.

Lin G, Tepp W, et al. Expression of the Clostridium botulinum A2 neurotoxin gene cluster proteins and characterization of the A2 complex. Applied and environmental microbiology. 2010; 76(1): 40–47. [PubMed: 19915042]

Malizio CJ, Goodnough MC, et al. Purification of Clostridium botulinum type A neurotoxin. Methods in molecular biology. 2000; 145:27–39. [PubMed: 10820714]

Rossetto O, Schiavo G, et al. SNARE motif and neurotoxins. Nature. 1994; 372(6505):415–416. [PubMed: 7984234]

Schantz EJ, Kautter DA. Standardized assay for clostridium botulinum toxins. Journal of the Association of Official Analytical Chemists. 1978; 61:96–99.

Schiavo G, Benfenati F, et al. Tetanus and botulinum-B neurotoxins block neurotransmitter release by proteolytic cleavage of synaptobrevin. Nature. 1992; 359(6398):832–835. [PubMed: 1331807]

Schiavo G, Malizio C, et al. Botulinum G neurotoxin cleaves VAMP/synaptobrevin at a single Ala-Ala peptide bond. Journal of biological chemistry. 1994; 269(32):20213–20216. [PubMed: 8051110]

Schiavo G, Matteoli M, et al. Neurotoxins Affecting Neuroexocytosis. Physiological Reviews. 2000; 80(2):717–766. [PubMed: 10747206]

Schiavo G, Rossetto O, et al. Identification of the nerve terminal targets of botulinum neurotoxin serotypes A, D, and E. Journal of biological chemistry. 1993; 268(32):23784–23787. [PubMed: 8226912]

Smith TJ, Lou J, et al. Sequence variation within botulinum neurotoxin serotypes impacts antibody binding and neutralization. Infection and immunity. 2005; 73(9):5450–5457. [PubMed: 16113261]

Vaidyanathan VV, Yoshino K, et al. Proteolysis of SNAP-25 isoforms by botulinum neurotoxin types A, C, and E: domains and amino acid residues controlling the formation of enzyme-substrate complexes and cleavage. Journal of neurochemistry. 1999; 72(1):327–337. [PubMed: 9886085]

Wang D, Baudys J, et al. Improved detection of botulinum neurotoxin type A in stool by mass spectrometry. Analytical biochemistry. 2011; 412(1):67–73. [PubMed: 21276417]

Wang D, Baudys J, et al. Improved Detection of Botulinum Neurotoxin Serotype A by Endopep-MS through Peptide Substrate Modification. Analytical Biochemistry. In press.

Washbourne P, Pellizzari R, et al. Botulinum neurotoxin types A and E require the SNARE motif in SNAP-25 for proteolysis. FEBS letters. 1997; 418(1–2):1–5. [PubMed: 9414082]

Werner SB, Passaro D, et al. Wound botulism in California, 1951–1998: recent epidemic in heroin injectors. Clinical infectious diseases. 2000; 31(4):1018–1024. [PubMed: 11049786]

Yamasaki S, Baumeister A, et al. Cleavage of members of the synaptobrevin/VAMP family by types D and F botulinal neurotoxins and tetanus toxin. Journal of biological chemistry. 1994; 269(17): 12764–12772. [PubMed: 8175689]

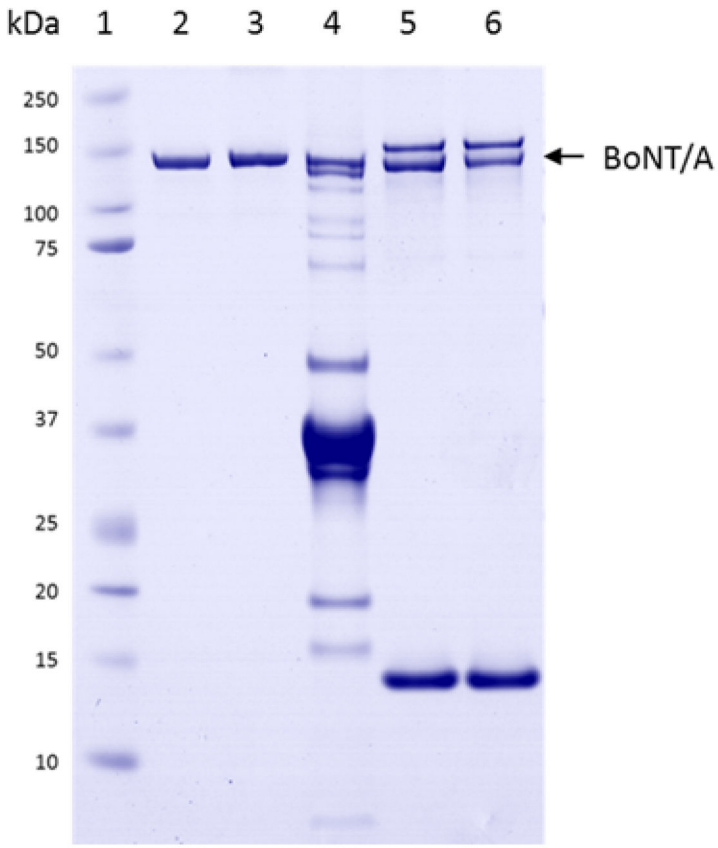

Figure 1.

1D gel image of the BoNT/A toxin samples. Lane 1: Molecular weight marker; Lane 2 and 3: purified BoNT/A1 and /A2. Lane 4: BoNT/A5 complex; Lane 5 and 6: A1 and A5 after extraction by toxin specific monoclonal antibody attached to magnetic beads. Bands at approximately 15 kDa and 155 kDa are associated with the antibody-coated streptavidin beads.

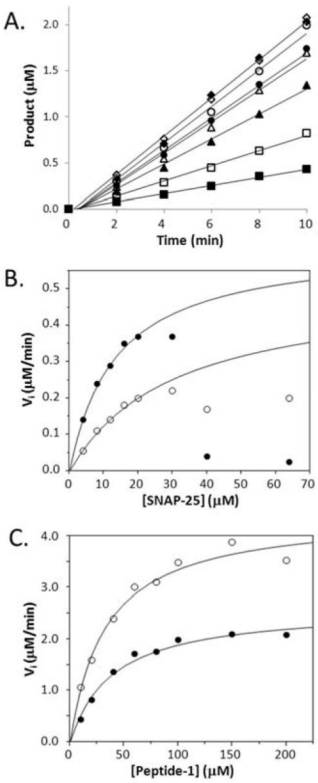

Figure 2.

A. A typical time-course plots for a set of BoNT/A5 catalyzed hydrolysis of Peptide-1 with various starting concentration of the substrate: 10 (■), 20 (□), 40 (▼), 60 (▽), 80 (●), 100 (○), 150 (◆) or 200 (◇) mM. B. and C. The plots of the reaction velocities as a function of the substrate concentration, measured as the slopes of the lines from the time-courses of the hydrolysis of SNAP-25 and the Peptide-1 cleaved by BoNT/A1 (○) or /A5 (●).

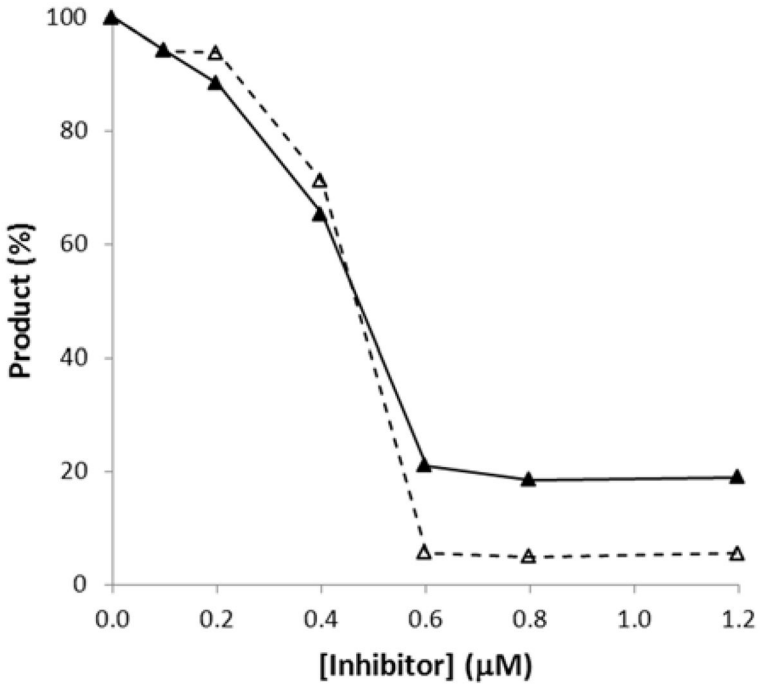

Figure 3.

Product inhibition on the cleavage of SNAP-25 by the BoNT/A subtype A1 (▼)and A5 (▽). The reactions were monitored by measuring the formation of the C-terminal product in the presence of the various concentrations of the purified N-terminal cleavage product (inhibitor).

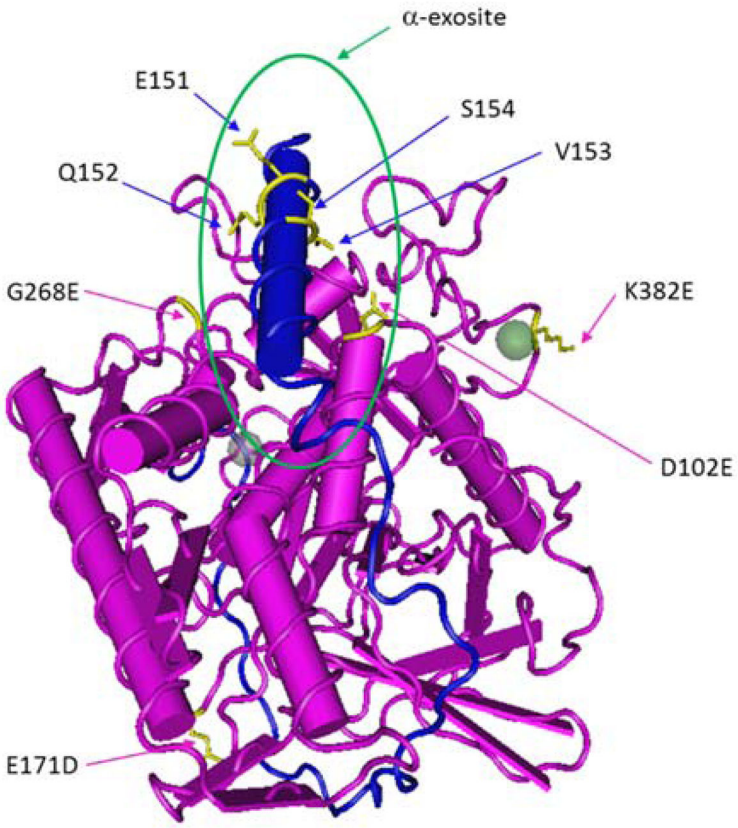

Figure 4.

Complex structure of the inactive light chain of BoNT/A1 (pink) and SNAP-$25_{141–204}$ (blue) (Breidenbach and Brunger 2004). The residues differentiated in BoNT/A5 and some selected residues in the peptide substrate are colored as yellow. Green circle represents the approximate location of α-exosite.

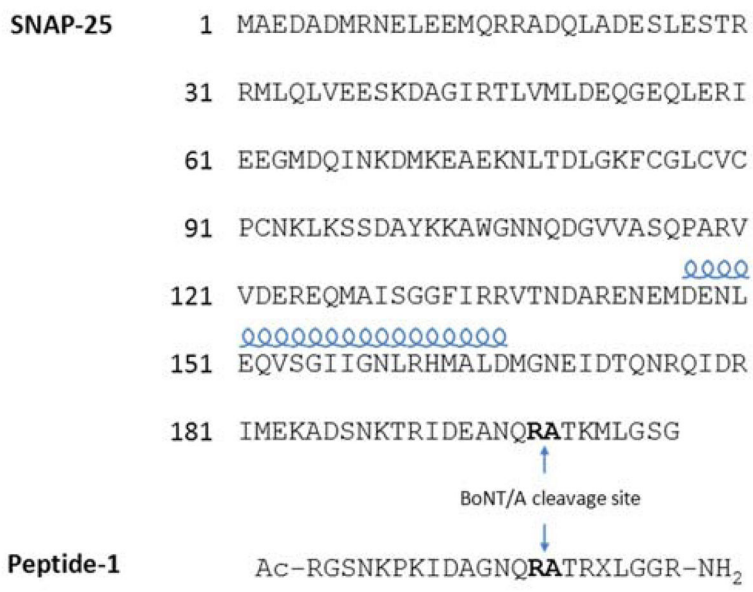

Scheme 1.

Sequences of SNAP-25 and an optimized peptide substrate for BoNT/A activity assay. Amino acid residues forming the scissile bond in the cleavage site are indicated by bold letters. X represents norleucine. The helical symbol above a selected region indicates the amino acid residues forming an α-helix in the crystal structure of the enzyme/substrate complex.

Table 1

Cleavage of the protein or peptide substrate by different BoNT/A subtypes*.

BoNT/A subtype	SNAP25		Peptide 1	
	Rate (μM/min)	Relative rate	Rate (μM/min)	Relative rate
A1	0.10 ± 0.01	1.0	0.09 ± 0.01	1.0
A2	0.05 ± 0.01	0.5	0.06 ± 0.01	0.7
A5	0.13 ± 0.01	1.3	0.06 ± 0.01	0.6

* Experiment condition: 1nM toxin, 4μM peptide 1 and SNAP25, 37°C for 10–60min.

Table 2

Kinetic parameters of the cleavage of the protein or peptide substrate by BoNT/A1 or A5.

Substrate	Toxin	K_m (μM)	k_{cat} (μM/min/nM toxin)	k_{cat}/K_m
SNAP-25	A1	30 ± 6	0.51 ± 0.07	0.017
	A5	13 ± 2	0.63 ± 0.04	0.048
	Purified A5	12 ± 2	0.51 ± 0.04	0.043
Peptide 1	A1	32 ± 5	4.44 ± 0.21	0.139
	A5	38 ± 6	2.62 ± 0.13	0.069

Table 3

Hydrolysis of the truncated SNAP-25 peptides by BoNT/A1 and /A5.*

Peptide	$Rate_{A1}$ (μM/min)	$Rate_{A5}$ (μM/min)	$Rate_{A5}/Rate_{A1}$
171–206	0.008	0.002	0.2
161–206	0.007	0.003	0.4
156–206	0.020	0.014	0.7
151–206	0.018	0.097	5.5
146–206	0.016	0.094	5.7
155–206	0.024	0.019	0.8
154–206	0.015	0.018	1.2
153–206	0.019	0.029	1.5
152–206	0.024	0.053	2.2
153–206/G155K	0.069	0.060	0.9
153–206/S154A	0.026	0.041	1.6
153–206/S154hS	0.016	0.023	1.4
153–206/S154K	0.065	0.057	0.9
153–206/S154R	0.060	0.058	1.0
153–206/V153A	0.029	0.033	1.1
153–206/V153K	0.076	0.053	0.7
153–206/V153D	0.013	0.051	4.0
153–206/V153E	0.016	0.050	3.2
153–206/E151A	0.036	0.082	2.3

* Cleavage reaction condition: 1nM toxin, 20uM peptide substrate, 37°C for 10 – 30 min.